



## Aerobic oxidation of benzyl alcohol in methanol solutions over Au nanoparticles: Mg(OH)<sub>2</sub> vs MgO as the support



Miguel Estrada<sup>a</sup>, Vinícius V. Costa<sup>b</sup>, Sergey Beloshapkin<sup>c</sup>, Sergio Fuentes<sup>d</sup>, Evgenii Stoyanov<sup>e</sup>, Elena V. Gusevskaya<sup>b,\*</sup>, Andrey Simakov<sup>d,\*\*</sup>

<sup>a</sup> Posgrado en Física de Materiales, CICESE, 22860 Ensenada, B.C., Mexico

<sup>b</sup> Universidade Federal de Minas Gerais, 31270-901 Belo Horizonte, MG, Brazil

<sup>c</sup> Materials & Surface Science Institute, University of Limerick, Limerick, Ireland

<sup>d</sup> Universidad Nacional Autónoma de México, Centro de Nanociencias y Nanotecnología, km. 107 Carretera Tijuana a Ensenada, C.P. 22860 Ensenada, B.C., Mexico

<sup>e</sup> University of California, Riverside, USA

### ARTICLE INFO

#### Article history:

Received 2 August 2013

Received in revised form

30 December 2013

Accepted 31 December 2013

Available online 8 January 2014

#### Keywords:

Gold catalysts

Oxidation

Benzyl alcohol

Magnesium oxide

Magnesium hydroxide

### ABSTRACT

Magnesium oxide and magnesium hydroxide materials containing supported gold nanoparticles (NPs), Au/Mg(OH)<sub>2</sub> and Au/MgO, were prepared from the commercial MgO through the deposition–precipitation (DP) method and characterized by XRD, XPS, HRTEM, FTIR spectroscopy and N<sub>2</sub> adsorption techniques. It was found that the starting MgO support was fully transformed into the Mg(OH)<sub>2</sub> phase during the DP procedure. A nearly complete dehydration of the magnesium hydroxide and formation of Au/MgO was achieved through the reductive treatment at 500 °C, whereas the treatment at 350 °C still resulted in the Au/Mg(OH)<sub>2</sub> material. The FTIR analysis showed a much higher ability of the Au/MgO surface to adsorb both benzyl alcohol and benzaldehyde (ca. 10 and 3 times, respectively), as compared to Au/Mg(OH)<sub>2</sub>. Probably for this reason, the Au/MgO catalyst exhibited ca. 50% higher catalytic activity in the aerobic oxidation/oxidative methylation of benzyl alcohol in the methanol solutions with respect to the amount of surface gold atoms as compared to the Au/Mg(OH)<sub>2</sub> catalyst, in spite of a larger size of the Au NPs. In addition, the thermal treatment of the catalyst at 500 °C to dehydrate the support allowed to suppress the undesired side reaction between benzyl alcohol and primarily formed benzaldehyde to give benzyl benzoate.

© 2014 Elsevier B.V. All rights reserved.

### 1. Introduction

The oxidation of alcohols represents a very important goal for synthetic organic chemistry since the resulting carbonyl compounds play a key role in various fields of chemical industry [1]. However, many currently used processes still involve stoichiometric oxidation reactions which generate vast quantities of effluents [2]. For these reasons, the development of appropriate catalysts for the oxidation of alcohols currently holds the attention of many research groups. It is especially attractive in the design of cheap processes to involve molecular oxygen as the oxidant due to its low cost (in comparison with other oxidants) and decrease in the byproduct formation and energy spent for the separation of target products. Various heterogeneous metal catalysts have been reported for the aerobic oxidation of alcohols [3–6], with gold

nanoparticles (NPs) being among the most promising ones [7–11]. Gold catalysts frequently show outstanding catalytic performance and total selectivity to carbonyl compounds.

The oxidation of primary alcohols over a supported metal catalyst likely begins with the formation of a metal alkoxide [4]. Typical side reactions are the aldol condensation and oligomerization [12–15]. The formation of strongly adsorbed byproducts, which can prejudice the activity and selectivity of the catalyst, has been frequently observed during the oxidation of alcohols over Pt-group metals [14]. A comparative study of the aqueous-phase aerobic oxidation of alcohols on supported Pt, Pd, and Au revealed that the latter metal was the most selective and the least prone to leaching [16–18]. High selectivity and stability of gold catalysts could be related with weak adsorption of reactants and products on gold particles as metallic gold is known to bind weakly most molecules including water [2,19].

Recently, we have found that the application of a basic support (MgO) for the preparation of gold catalysts permits to perform effectively the oxidative methylation of benzyl alcohol as well as the oxidation of a wide range of other alcohols in the absence of an additional base co-catalyst [20]. The present paper is devoted to

\* Corresponding author.

\*\* Corresponding author. Tel.: +52 6461744602; fax: +52 6461744603.

E-mail addresses: [elena@ufmg.br](mailto:elena@ufmg.br) (E.V. Gusevskaya), [andrey@cbyn.unam.mx](mailto:andrey@cbyn.unam.mx), [andrey.cnyn@gmail.com](mailto:andrey.cnyn@gmail.com) (A. Simakov).

the further analysis of the support effect on the transformation of alcohols over gold catalysts prepared using the commercial MgO as the starting support. It is well known that MgO could be easily converted into Mg(OH)<sub>2</sub> in the presence of water, especially under acidic conditions [21]. Usually the hydrolysis of MgO occurs during the gold deposition by DP technique from aqueous solutions [22]. However, thermal treatment of the material at 500 °C permits to decompose Mg(OH)<sub>2</sub> and re-form MgO [23]. The aim of the present work was to study the effect of the support transformation from Mg(OH)<sub>2</sub> to MgO on the state of gold and its activity in the oxidation of benzyl alcohol with molecular oxygen in methanol solutions. We have also studied the interaction of key components of the reaction media with the Au/MgO and Au/Mg(OH)<sub>2</sub> catalysts by IR spectroscopy.

## 2. Experimental

### 2.1. Catalyst preparation

Gold (2.6 wt.%) was supported by deposition–precipitation using HAuCl<sub>4</sub> as a gold precursor and urea as a precipitation agent as in [24]. MgO (4.0 g, Mallinckrodt) was added to an aqueous solution (400 mL) of HAuCl<sub>4</sub> ( $1.6 \times 10^{-3}$  M) and urea (0.42 M). The initial pH of the solution was ca. 2. The suspension was vigorously stirred at 80 °C for 4 h. Then, the solid material was filtered and washed with ammonium hydroxide (25.0 M) for 30 min. The last procedure developed in [25] is quite effective to stabilize small gold NPs. After stirring with ammonium hydroxide, the pH of the solution was ca. 10. Finally, the sample was washed with water until the pH of the solution reached the value of 7, then filtered, and dried at room temperature for 24 h. The freshly prepared sample denoted as Au/Mg-F was used to obtain gold supported on Mg(OH)<sub>2</sub> via the reduction in the mixture of H<sub>2</sub> (5 vol.%) in He (a total flow rate of 50 mL/min) at a heating rate of 20 °C/min up to 350 °C. The obtained sample was denoted as Au/Mg-350. For the preparation of gold supported on MgO, the Au/Mg-F sample was reduced in the same gas mixture at 500 °C at the same heating rate and denoted as Au/Mg-500.

### 2.2. Catalyst characterization

The specific surface area and pore size distribution were determined according to the BET method by nitrogen adsorption measurements in a Tri-Star III device. Before analysis the samples were treated in a vacuum ( $10^{-3}$  torr) at 300 °C for 4 h.

X-ray diffraction (XRD) analysis was carried out with a Philips X'pert diffractometer equipped with a curved graphite monochromator applying a CuK<sub>α</sub> ( $\lambda = 0.154$  nm) radiation.

Photoelectron spectroscopy (XPS) data were obtained by a Kratos AXIS 165 spectrometer using a monochromatic AlK<sub>α</sub> radiation ( $h\nu = 1486.58$  eV) and fixed analyzer pass energy of 20 eV. All measured binding energies (BE) were referred to C 1s line of adventitious carbon at 284.8 eV. The deconvolution of spectra was carried out with a background estimation using the Shirley software.

Gold content (2.6 wt.%) was determined by inductively coupled plasma atomic emission spectroscopy (ICP-AES) on a Varian Liberty 110 instrument. Solid samples pretreated at 350 °C in Ar flow for 30 min were first digested at room temperature in HF for 12 h and then in a mixture of HCl and HNO<sub>3</sub> for 30 min. The solution obtained was diluted with deionized water and analyzed.

High-resolution transmission electron microscopy (HRTEM) was performed with a JEOL 2010 microscope. The sample was dispersed by ultrasonic in isopropanol and supported on a copper grid covered with a carbon film. To determine the mean diameter of gold

particles, more than 200 particles were chosen. The mean diameter ( $d_m$ ) of particles was calculated using the following formula:

$$d_m = \frac{\sum_i (x_i d_i)}{\sum_i x_i},$$

where  $x_i$  is the number of particles with diameter  $d_i$ .

A spectrometer Nexus-760 with a DTGS detector and in situ cell from Harrick was used in the diffuse reflectance Fourier transform (DRIFT) mode for analysis of benzyl alcohol and benzaldehyde adsorbed at 30 °C. Before the benzyl alcohol or benzaldehyde adsorption the samples were heated in situ in Ar (a flow rate of 20 mL/min, ultra high purity grade from Infra) with a temperature increase up to 350 °C at a ramp rate of 20 °C/min. Then temperature was decreased to 30 °C. The spectra of the samples before the benzyl alcohol or benzaldehyde adsorption were recorded using the spectrum of mirror as a reference with a resolution of 4 cm<sup>-1</sup>. The adsorption was carried out until the sample saturation in a flowing mixture of benzyl alcohol (0.01 vol.%) or benzaldehyde (0.16 vol.%) and Ar (a total flow rate of 20 mL/min) for about 1 h. After the stabilization of FTIR spectra the samples were flushed by Ar at 30 °C for 30 min to remove the gas phase or weakly adsorbed benzyl alcohol or benzaldehyde. In order to study a thermal stability of the adsorbed benzyl alcohol and benzaldehyde the catalyst sample was heated from 30 °C up to 90 °C at a ramp rate of 5 °C/min in the Ar flow (20 mL/min). Before the entrance to the FTIR cell, Ar was dried by passing through a trap cooled at -20 °C by the mixture of *n*-isopropanol and liquid nitrogen. During the adsorption and thermal desorption of benzyl alcohol or benzaldehyde the spectra were recorded in the Kubelka-Munk unites (32 scans) using a spectrum of the catalyst sample before adsorption as a reference. The temperature of the sample within a DRIFT cell during the thermal desorption was precisely measured using a thin thermocouple with a fast response. In preliminary experiments, no significant temperature gradient through a catalyst bed was found at the same ramp rate of 5 °C/min.

### 2.3. Catalytic oxidation experiments

The reactions were carried out in a stainless steel reactor equipped with a magnetic stirrer. In a typical run, a mixture of benzyl alcohol (2.5 mmol), methanol (2 mL), and the catalyst (10 mg; 1.3 μmol of Au; 0.05 mol%) was transferred in the reactor. The reactor was pressurized with oxygen to the total pressure of 10 atm and placed in an oil bath; then, the solution was intensively stirred at 110 °C for the reported time. The reactions were followed by gas chromatography (GC) (Shimadzu 17 instrument, Carbowax 20M capillary column). At appropriate time intervals, stirring was stopped and after catalyst settling aliquots were taken and analyzed by GC. The structures of the products were confirmed by GC/MS (Shimadzu QP2010-PLUS instrument, 70 eV).

## 3. Results and discussion

The phase composition of the prepared samples was studied by XRD. It was shown that XRD patterns of the freshly prepared Au/Mg-F sample and Mg(OH)<sub>2</sub> reference sample are practically equal (Fig. 1). Thus, during the gold deposition by the DP procedure the starting MgO was completely transformed into Mg(OH)<sub>2</sub> via the interaction with water [21]. The process seemed to be accelerated by the presence of the strong HAuCl<sub>4</sub> acid at the beginning of the DP procedure. The thermal treatment of the Au/Mg-F sample at 350 °C in a hydrogen flow did not lead to the decomposition of Mg(OH)<sub>2</sub> into MgO. It should be noted that no reflections corresponding to Au metal nanoparticles (Au NPs) have been detected in the XRD pattern of both the Au/Mg-F and Au/Mg-350 samples. This

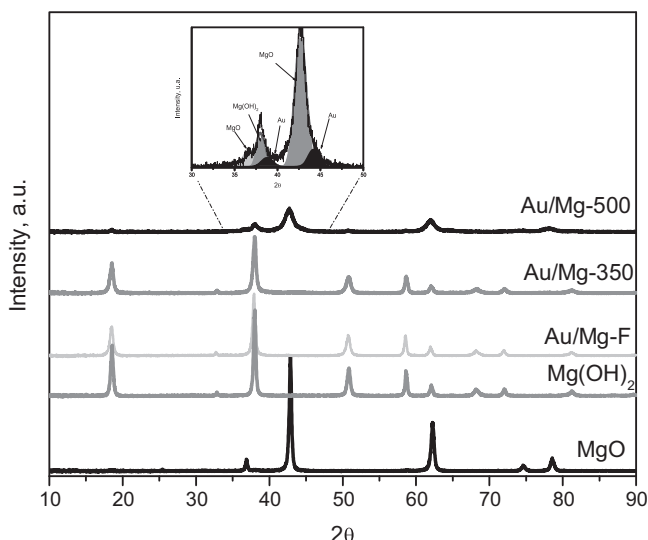


**Fig. 1.** XRD patterns for the catalyst samples after thermal treatment in hydrogen at 350 (Au/Mg-350) and 500 °C (Au/Mg-500) and for the reference samples (the freshly prepared sample Au/Mg-F, magnesium oxide and magnesium hydroxide). Contribution of different phases for the Au/Mg-500 sample is illustrated by insertion.

could be explained by the relatively small size of the Au NPs, which really has been found by TEM for Au/Mg-350 (3.5 nm, see below).

On the other hand, the XRD pattern for the Au/Mg-500 sample showed mainly the reflections of MgO with larger peak widths compared to those of the reference MgO sample. Thus, the thermal treatment of the Au/Mg-F sample at 500 °C resulted in a practically complete dehydration of the Mg(OH)<sub>2</sub> phase and expectable appearance of the MgO phase. Indeed, it was reported in [26] that Mg(OH)<sub>2</sub> could be converted into MgO by thermal treatment at 480 °C. The detailed analysis of the XRD pattern for the Au/Mg-500 sample in the interval of 30–50 (2 $\Theta$ ) (shown by insertion in the Fig. 1) revealed the reflections related to the presence of a residual Mg(OH)<sub>2</sub> phase and metallic Au nanoparticles.

The estimated values of coherently scattering domains for different phases are presented in Table 1. These values could be used for estimation of crystal size for MgO, Mg(OH)<sub>2</sub> and Au NPs. The size of the Mg(OH)<sub>2</sub> crystals in Au/Mg-350 was comparable with that for the initial MgO, while a thermal decomposition of Mg(OH)<sub>2</sub> resulted in the reformation of MgO species of a much smaller size in the Au/Mg-500 sample. The analysis of the reflections related to Au NPs using the Scherer's equation gave rough estimation of a size of about 14 nm for the Au NPs in the Au/Mg-500 sample.

The transformation of MgO into Mg(OH)<sub>2</sub> and back to MgO during the preparation of gold catalysts significantly affected the pore structure of the support. The distribution of pore size for the obtained samples is pictured in Fig. 2. The initial MgO was characterized with relatively small pores and a high surface area

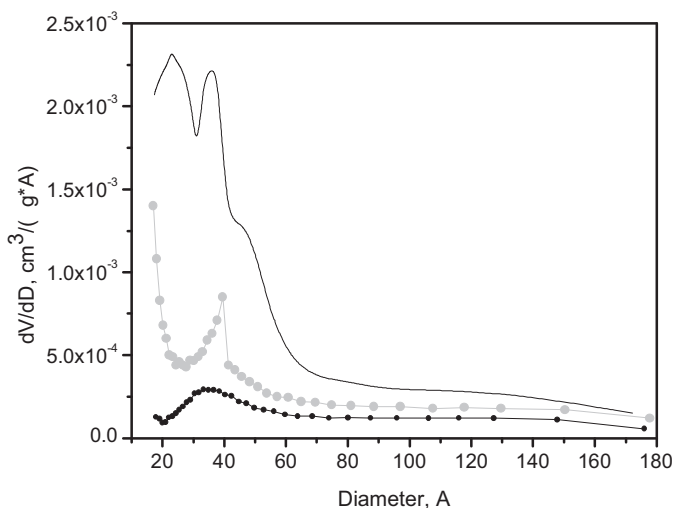


**Fig. 2.** Distribution of pores for the initial MgO (thin black line) and for Au/Mg-350 (gray circles), Au/Mg-500 (black circles) catalysts.

(see Table 1). The formation of Mg(OH)<sub>2</sub> during the gold deposition resulted in the dramatic decrease of the surface area and pore volume. The thermal decomposition of Mg(OH)<sub>2</sub> into MgO during the calcination of the Au/Mg-350 sample at 500 °C was accompanied with a further decrease of the pore volume and surface area apparently due to the partial agglomeration of the formed MgO particles.

The surface composition of the prepared samples was evaluated by the XPS analysis. The 1s O XP spectra of the Au/Mg-350 and Au/Mg-500 samples are presented in Fig. 3. Oxygen species located on the surface of these samples were characterized with the peaks of a wide width. A deconvolution procedure revealed the presence of the peaks centered at 531.8 and 531.2 eV for Au/Mg-350 (Fig. 3, bottom) and the peaks centered at 531.5 and 529.4 eV for Au/Mg-500 (Fig. 3, top). The peak at 531.8 eV was assigned to carbonates formed due to the CO<sub>2</sub> adsorption from the gas phase [27]. The peak at 531.5 eV was assigned to the presence of the MgCO<sub>3</sub>–Mg(OH)<sub>2</sub> hydrated phase on the sample surface, while the peak at 531.2 eV to the Mg(OH)<sub>2</sub> phase according to [28]. The thermal treatment at 500 °C significantly decreased a relative content of carbonates on the surface of Au/Mg-500 and led to the appearance of a new peak

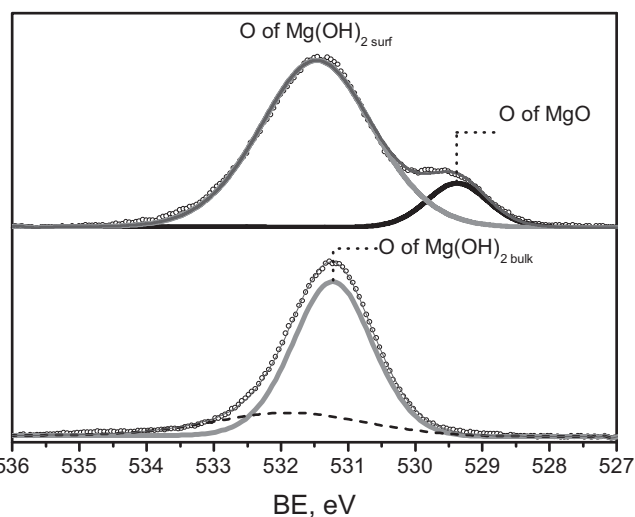


**Fig. 3.** 1s O XPS spectra for the Au/Mg-350 (bottom) and Au/Mg-500 (top) samples. Deconvolution curves correspond to oxygen species of: MgO (solid black line), Mg(OH)<sub>2</sub> (solid gray line) and carbonates (dash black line).

**Table 1**

Estimated values of the coherently scattering domains (CSD) obtained from the XRD patterns using the Scherer's equation for magnesium oxide, magnesium hydroxide and Au metal particles.

Sample	Phase	Crystal direction	Size of CSD, nm	SBET, m <sup>2</sup> /g
MgO	MgO	200	26	105
Au/Mg-350	Mg(OH) <sub>2</sub>	111	23	41
	MgO	200	n.d.	
	Au	111	n.d.	
Au/Mg-500	Mg(OH) <sub>2</sub>	111	14	17
	MgO	200	7	
	Au	111	14	

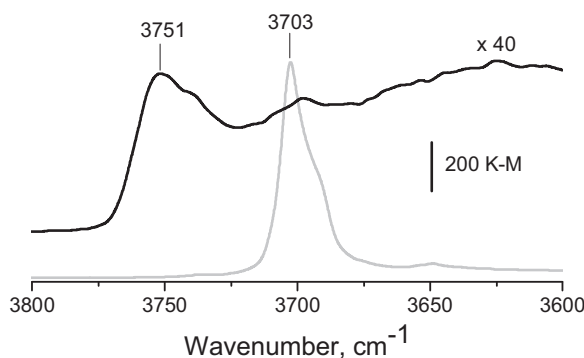


**Fig. 4.** IR spectra of the Au/Mg-350 (gray line) and Au/Mg-500 (black line) samples recorded at 30 °C in an Ar flow after the thermal in situ treatment in an Ar flow up to 350 °C with a ramp rate of 20 °C/min.

at 529.4 eV assigned to MgO [28] (Fig. 3, top). The presence of the Mg(OH)<sub>2</sub> species on the surface of Au/Mg-500 can be explained by the incomplete decomposition of the Mg(OH)<sub>2</sub> phase during the sample heating at 500 °C and/or by a partial hydration of MgO during an exposure of the sample to the atmosphere [22]. A combined analysis of the XPS (surface technique) and XRD (bulk technique) data suggests that only a part of the surface layer in the Au/Mg-500 sample consists of the Mg(OH)<sub>2</sub> phase. It is important to note that a partial transformation of MgO into Mg(OH)<sub>2</sub> in Au/Mg-500 can be expected during the catalytic tests of this material in the oxidation of alcohols because the catalyst can interact with a residual water present in reaction solutions. The samples after the reaction have been analyzed by FTIR spectroscopy. The spectra of both spent catalysts were similar to those before the catalytic tests, with no significant amounts of Mg(OH)<sub>2</sub> being found in the spent Au/Mg-500 sample (see Supporting Information, Fig. 1).

The surface of the Au/Mg-350 and Au/Mg-500 samples was also explored by IR spectroscopy. Spectra were collected just after the thermal treatment of the samples in a IR cell in Ar without their contact with air (Fig. 4). The spectrum of the Au/Mg-350 sample developed highly intensive band of OH stretch vibrations at 3702 cm<sup>-1</sup> related to both surface and bulk OH groups of the Mg(OH)<sub>2</sub> phase [29,30]. A thermal treatment at 500 °C led to the drastic decrease in the intensity of this band (residual intensity is less than 1%) and appearance of a new band at 3751 cm<sup>-1</sup> assigned to the νOH of surface hydroxyl groups of MgO [29]. Thus, the IR data also evidenced the almost complete decomposition of Mg(OH)<sub>2</sub> to MgO during the sample treatment at 500 °C.

The different thermal treatment of the samples affected also the size of the Au NPs. TEM images of Au/Mg-350 and Au/Mg-500 are presented in Fig. 5. For both samples, Au NPs were indicated in the TEM micrographs mostly as hexagonal dark features. A mean diameter for the Au NPs in Au/Mg-350 and Au/Mg-500 was found to be equal to 3.4 and 6.5 nm, respectively. Thus, the increase in the temperature of the thermal treatment provokes the migration and agglomeration of the Au NPs. Indeed, it has been reported that migration of small Au NPs could begin at relatively low temperatures [31]. On the other hand, the changes of the support surface during the Mg(OH)<sub>2</sub> transformation into MgO should be taken into account as well. It is known that even the partial dehydration of Mg(OH)<sub>2</sub> results in the formation of oxygen vacancies [21] which can serve as sites for the Au species stabilization. The thermal treatment leads to the distortion of these structures and the formation of free Au species which readily agglomerate into Au NPs. The growth of Au NPs after the thermal treatment at 500 °C results in a significant decrease (almost two times) of the relative content of surface Au atoms in NPs. In principle, that could result in the decrease in the catalytic activity of Au/Mg-500 compared to Au/Mg-350. In addition, the hydroxylated support (Mg(OH)<sub>2</sub>) is characterized with an enhanced supply of active oxygen, as it has been shown for the CO oxidation on colloidal Au particles deposited on Mg(OH)<sub>2</sub> [32], which can also affect the catalytic activity of the material in alcohol oxidations.

To clarify a chemical state of the gold species formed on the catalyst surface, the Au/Mg-350 and Au/Mg-500 samples were analyzed by X-ray photoelectron spectroscopy (XPS). The XP spectra for the Mg 2s and Au 4f regions are presented in Fig. 6. The spectra for Au 4f showed two doublets of two spin-orbit components separated by 3.67 eV, i.e., Au 4f<sub>7/2</sub> and Au 4f<sub>5/2</sub>, which could be attributed to metallic gold species and Au<sup>+</sup> cations [33]. It should be noted that the fraction of the Au<sup>+</sup> cations is practically equal for both samples. However, the content of the Au<sup>+</sup> cations cannot be evaluated precisely because of overlapping of the gold peaks with the highly intensive peak of Mg. The comparison of the intensity of gold peaks and the Mg peak reveals that the relative content of the surface gold species is significantly lower in Au/Mg-500 than in Au/Mg-350. This could be explained by the agglomeration of the Au NPs in the Au/Mg-500 sample at thermal treatment confirmed by TEM.

The nature of the support (MgO or Mg(OH)<sub>2</sub>) can also affect the interaction of main components of the reaction media with the catalyst surface. The capacity of the Au/Mg-350 and Au/Mg-500 samples to adsorb benzyl alcohol and benzaldehyde was estimated from the intensity of the DRIFT spectra of these compounds adsorbed at 30 °C (Fig. 7), because the frequencies of the

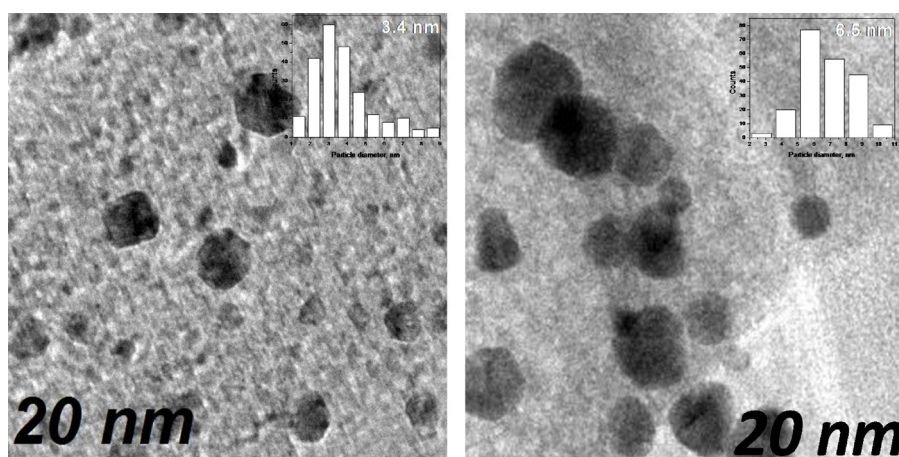


**Fig. 5.** TEM images and the histograms of the gold particle size distribution for the Au/Mg-350 (left) and Au/Mg-500 (right) samples.

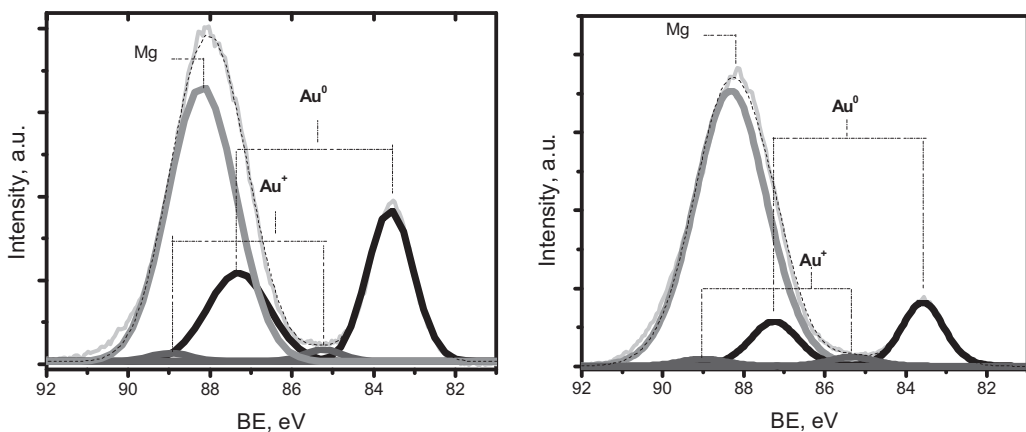


**Fig. 6.** The experimental XP spectra (gray line) and the results of fitting of the Mg 2s (dark gray line) and Au 4f region (solid black lines) for the Au/Mg-350 (left) and Au/Mg-500 (right) catalysts.

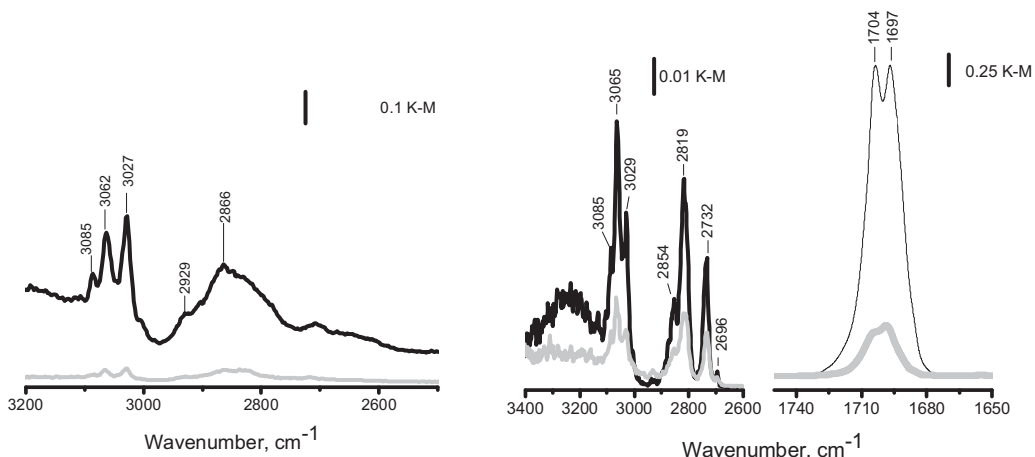


**Fig. 7.** IR spectra of benzyl alcohol (left) and benzaldehyde (right) adsorbed at 30 °C on the Au/Mg-350 (gray lines) and Au/Mg-500 (black lines) samples after flushing the saturated samples with Ar for 30 min.

characteristic bands in their spectra did not change significantly for both catalysts (Table 2). It was found that the intensities of the absorption bands for benzyl alcohol and benzaldehyde adsorbed on Au/Mg-500 were ca. 10 and 3 times, respectively, higher than for those adsorbed on Au/Mg-350. We suppose that such a dramatic difference cannot be explained only by the possible different scattering properties of the samples. Thus, a capacity of the MgO surface to adsorb benzyl alcohol and benzaldehyde seems to be much superior to that of  $\text{Mg}(\text{OH})_2$ .

To determine how strong the adsorbed molecules are attached to the surface, it is useful to compare their spectra with those of “free” (undisturbed) molecules in  $\text{CCl}_4$  solutions. The bands of the aromatic CH stretch vibrations for the adsorbed molecules ( $3083, 3066$  and  $3028 \text{ cm}^{-1}$ ) and for those dissolved in  $\text{CCl}_4$  [34–36]

practically coincide (not shown in Table 2). However, the stretch vibrations of the  $\text{CH}_2$  group of the adsorbed benzyl alcohol are distinctly red shifted as compared to that dissolved in  $\text{CCl}_4$  [34,35] (Table 2). This result indirectly indicates that benzyl alcohol is bounded with the catalyst surface via its OH group that leads to some withdrawing the electron density from the  $\text{CH}_2$  group and decreasing its stretch frequencies. Benzaldehyde bonding via the carbonyl group to the surface results in slight red shifts of the  $\nu(\text{C=O})$  frequency of the adsorbed molecules (Table 2) as compared to those dissolved in  $\text{CCl}_4$  [36]. The influence of the catalyst nature on the frequencies of the characteristic bands of the adsorbed benzyl alcohol ( $\nu\text{CH}_2$ ) and benzaldehyde ( $\nu\text{CO}$ ) is negligible as the differences are within the experimental error (Table 2). The relative strength of benzyl alcohol and benzaldehyde adsorption on the

**Table 2**

The stretch frequencies ( $\text{cm}^{-1}$ ) of the  $\text{CH}_2$  group of benzyl alcohol and  $\text{C=O}$  group of benzaldehyde, which are influenced under absorption of its molecules on Au/Mg-350 and Au/Mg-500. The frequencies of the undisturbed molecules, dissolved in  $\text{CCl}_4$ , are given for comparison.

	$\text{CCl}_4^{\text{a}}$	$\text{Au/Mg-350}^{\text{b}}/\Delta^{\text{d}}$	$\text{Au/Mg-500}^{\text{c}}/\Delta^{\text{d}}$	Assignments
Benzyl alcohol	2935	2927/8	2929/6	$\nu_{\text{as}}\text{CH}_2$
	2876	2866/10	2866/10	$\nu_{\text{s}}\text{CH}_2$
Benzaldehyde	1709	1706/3, 1698/11	1704/5, 1697/12	$\nu(\text{C=O})$

<sup>a</sup> Dissolved in  $\text{CCl}_4$  benzyl alcohol [35] and benzaldehyde [36].

<sup>b</sup> Adsorbed on Au/Mg-350.

<sup>c</sup> Adsorbed on Au/Mg-500.

<sup>d</sup> The difference in frequency for the molecules dissolved in  $\text{CCl}_4$  and adsorbed on the surface.

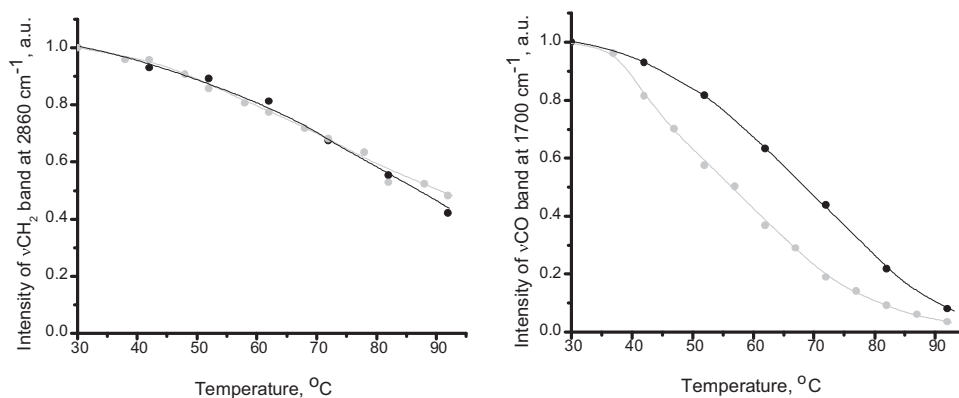


**Fig. 8.** Changes of the relative intensity of the IR bands during the thermal treatment of the Au/Mg-350 (gray symbols and line) and Au/Mg-500 (black symbols and line) samples at a ramp rate of 5 °C/min in an Ar flow after the sample saturation with benzyl alcohol (left) and benzyl aldehyde (right) at 30 °C.

**Table 3**

Oxidation of benzyl alcohol (**1a**) catalyzed by Au/Mg-350 and Au/Mg-500 in methanol solution.<sup>a</sup>

Catalyst	Time (h)	Conversion (%)	Product selectivity (%)			TOF <sup>b</sup> (h <sup>-1</sup> )
			Aldehyde <b>1b</b>	Ester <b>1c</b>	Ester <b>1d</b>	
Au/Mg-350	1	38	67	25	8	2155
	2	55	55	35	10	
	4	73	47	51	11	
	10	96	33	57	10	
Au/Mg-500	1	30	89	11	0	3259
	2	44	82	18	0	
	4	58	76	23	0	
	10	78	66	33	0	

<sup>a</sup> Conditions: benzyl alcohol (2.5 mmol); catalyst [10 mg, 2.6 wt.% (1.3 μmol) of Au]; methanol (2 mL); 110 °C, 10 atm (O<sub>2</sub>). Conversion and selectivity were determined by GC.

<sup>b</sup> Initial rate of the substrate conversion (initial turnover frequency) per mol of the surface Au. The surface amounts of Au correspond to 33.9% of the total amounts for Au/Mg-350 and 17.7% for Au/Mg-500 (estimation is based on the average particle diameter of 3.4 and 6.5 nm, respectively).

catalysts was estimated via the study of their thermal desorption from the catalyst surface.

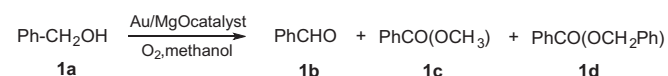
The band intensity of the aromatic CH stretch vibrations (which represent the surface density of the adsorbed compounds) decreased in a linear proportion with the intensity of the νCH<sub>2</sub> bands of benzyl alcohol and ν(C=O) band of benzaldehyde for both samples within the temperature interval studied (30–90 °C). This implies that the thermal desorption is not accompanied with the formation of new compounds on the surface. Therefore, the decrease in the intensity of the νCH<sub>2</sub> and ν(C=O) bands represents the decrease in the surface density of benzyl alcohol and benzaldehyde, respectively (Fig. 8). For comparison of the surface density change with temperature for different samples, the intensities of the aliphatic and carbonyl bands of the benzyl alcohol and benzaldehyde adsorbed on Au/Mg-350 and Au/Mg-500 were normalized to 1 at the starting temperature of 30 °C. For such low temperatures (30–90 °C) it can be assumed that the size of the sample particles does not change significantly; therefore, diffuse light scattering for both samples should be constant. To monitor the relative changes in the spectra intensity (i.e., the surface density of the adsorbed compounds) vs. temperature the normalization procedure with the exclusion of the specific diffuse light scattering was applied.

It has been shown that the desorption of benzyl alcohol proceeds similarly for both samples confirming that the binding strength of the adsorbed benzyl alcohol with both catalysts is similar. Thus, the higher adsorption of benzyl alcohol on the Au/Mg-500, as compared to that on Au/Mg-350, seems to be determined by high density of the adsorption sites on Au/Mg-500 rather than their adsorption strength. On the other hand, the tendency found for benzaldehyde was different (Fig. 8, right): the desorption from Au/Mg-500 was

slower than from Au/Mg-350. Therefore, benzaldehyde seems to interact stronger with Au/Mg-500 than with Au/Mg-350.

The catalytic activity of the Au/Mg-350 and Au/Mg-500 catalysts was tested in the oxidation of benzyl alcohol (**1a**) with molecular oxygen in methanol solutions. The results are presented in Table 3. Both catalysts effectively promoted the oxidation and oxidative esterification of benzyl alcohol in the absence of any co-catalysts or additives. The reaction resulted in two major products: benzaldehyde **1b** and methyl benzoate **1c** (Scheme 1). The combined selectivity for these two products was 90–100%, with only small amounts of benzyl benzoate **1d** being detected in the reaction over Au/MgO-350. Relative amounts of **1b** and **1c** depended on the reaction time with the selectivity for ester **1c** being increased at the end of the reaction.

Methyl benzoate and benzyl benzoate are formally the products of the esterification of benzoic acid with methanol and benzyl alcohol, respectively. However, within the currently accepted mechanism their formation occurs through the dehydrogenation of hemiacetals considered as key intermediates of the process [37–40]. The first reaction step is the oxidation of the alcohol into benzaldehyde. Then, the corresponding hemiacetals are suggested to be formed by the condensation of benzaldehyde and methanol or benzyl alcohol.



**Scheme 1.** Oxidation of benzyl alcohol **1a** into benzaldehyde **1b**, methyl benzoate **1c** and benzyl benzoate **1d**.

The conversion of benzyl aldehyde occurred faster with the Au/Mg-350 catalyst than with Au/Mg-500 (Table 3). However, considering the average diameter of the Au NPs in both samples (3.4 and 6.5 nm for Au/Mg-350 and Au/Mg-500, respectively) it becomes clear that, accordingly to initial reaction rates, gold species supported on the MgO surface (Au/Mg-500) are ca. 50% more active in the oxidation of benzyl alcohol as compared to those on Mg(OH)<sub>2</sub> (Au/Mg-350). The initial turnover frequencies (TOFs) presented in Table 3 were calculated as a ratio between the initial rates of the substrate conversion and the surface amounts of Au, i.e., with respect to the fraction of gold atoms located on the surface of the gold particles which were, therefore, accessible for the substrate. The surface amounts of Au (33.9% of the total amounts for Au/Mg-350 and 17.7% for Au/Mg-500) were estimated based on the average particle diameter determined by TEM as the study by X-ray absorption spectroscopy has confirmed that the starting Au/Mg-350 material no contains appreciable amounts of the Au particles smaller than 1 nm [20]. The leaching of Mg and Au was evaluated by the ICP analysis of the reaction solutions after the 10 hour reactions. No Au and small quantities of Mg were found: 70 and 150 ppm for the Au/Mg-350 and Au/Mg-500 samples, respectively. The presence of basic magnesium in the reaction solutions in principle could favor the reaction. The spent catalysts were examined by FTIR. No phase transformations in both catalysts were detected after the catalytic tests (see Supporting Information).

Thus, under the same reaction conditions, the catalytic activity of the surface Au species supported on MgO was at least 50% higher than that of those supported on Mg(OH)<sub>2</sub> in spite of both small size of Au NPs on Au/Mg-350 and the expected enhanced ability of the hydroxylated support, Mg(OH)<sub>2</sub>, to supply an active oxygen [41]. A plausible explanation for these results could be the much higher capacity of the dehydrated MgO surface (Au/Mg-500) to adsorb and, therefore, to activate the substrate, benzyl alcohol, on the supported Au NPs. Thus, a decisive parameter to determine the catalytic activity of the material obtained from the commercial MgO seems to be the ability of the surface to interact with benzyl alcohol enhancing the substrate activation over the surface Au species. It should be noted that the reaction over the Au/Mg-350 catalyst results in the formation of benzyl benzoate **1d** in appreciable amounts (ca. 10%), differently from that over Au/Mg-500, which could also be related to the adsorption properties of the catalyst surface.

#### 4. Conclusions

Gold catalysts based on MgO are effective heterogeneous catalysts for the aerobic oxidation and oxidative esterification of alcohols in the absence of the additional base co-catalyst probably due to the partial leaching of Mg. However, it has been found that MgO is completely transformed into Mg(OH)<sub>2</sub> during the catalyst preparation through the conventional deposition–precipitation method. The dehydration of the hydroxide back to MgO can be achieved through the reductive treatment of the material at 500 °C, whereas the treatment at 350 °C still results in Mg(OH)<sub>2</sub>. However, a temperature increase during the catalyst treatment leads to larger Au NPs: the average particle diameter was found to be 6.5 nm in Au/Mg-500 whereas 3.4 nm in Au/Mg-350. The MgO surface containing Au NPs posses a much higher ability to adsorb benzyl alcohol and benzaldehyde (ca. 10 and 3 times, respectively), as compared to Mg(OH)<sub>2</sub>. Probably for this reason, Au NPs supported on MgO show ca. 50% higher catalytic activity in the aerobic oxidation of benzyl alcohol with respect to the amounts of surface gold atoms as compared to Mg(OH)<sub>2</sub>. In addition, the dehydration of the support allows to suppress the undesired side reaction between benzyl alcohol and benzaldehyde to give benzyl benzoate.

The catalytic efficiency of gold nanoparticles depends on their size and the affinity of the support to stabilize key reaction components as well. In some cases, as it has been found in the present work, the impact of the support can be determinative.

#### Acknowledgments

The authors thank E. Flores, P. Casillas, V. Garcia, M. Sainz, F. Ruiz, E. Aparicio, M. Vega and J. Peralta for technical support. This research project was partially supported by CONACyT (México) and PAPIIT-UNAM (México) through Grants 179619 and 203813, respectively and by CNPq, CAPES, FAPEMIG and INCT-Catálise (Brazil).

#### Appendix A. Supplementary data

Supplementary data associated with this article can be found, in the online version, at <http://dx.doi.org/10.1016/j.apcata.2013.12.039>.

#### References

- [1] D. Romano, R. Villa, F. Molinari, *ChemCatChem* 4 (2012) 739–749.
- [2] R.A. Sheldon, I.W.C.E. Arends, A. Dijksman, *Catal. Today* 57 (2000) 157–166.
- [3] K. Mori, T. Hara, T. Mizugaki, K. Ebitani, K. Kaneda, *J. Am. Chem. Soc.* 126 (2004) 10657–10666.
- [4] T. Mallat, A. Baiker, *Chem. Rev.* 104 (2004) 3037–3058.
- [5] T. Nishimura, N. Kakiuchi, M. Inoue, S. Uemura, *Chem. Commun.* 14 (2000) 1245–1246.
- [6] K. Yamaguchi, N. Mizuno, *Angew. Chem. Int. Ed.* 41 (2002) 4538–4541.
- [7] L. Prati, M. Rossi, *J. Catal.* 176 (1998) 552–560.
- [8] C. Della Pina, E. Falletta, L. Prati, M. Rossi, *Chem. Soc. Rev.* 37 (2008) 2077–2097.
- [9] G.J. Hutchings, *Chem. Commun.* 10 (2008) 1148–1164.
- [10] A. Corma, H. Garcia, *Chem. Soc. Rev.* 37 (2008) 2096–2126.
- [11] V.R. Choudhary, D.K. Dumbre, *Catal. Commun.* 13 (2011) 82–86.
- [12] M.I.A. Khan, Y. Miwa, S. Morita, J. Okada, *Chem. Pharm. Bull.* 29 (1981) 1795–1802.
- [13] J.W. Nicoletti, G.M. Whitesides, *J. Phys. Chem.* 93 (1989) 759–767.
- [14] T. Mallat, A. Baiker, *Appl. Catal. A* 79 (1991) 41–58.
- [15] J.M. Bonello, F.J. Williams, A.K. Santra, R.M. Lambert, *J. Phys. Chem. B* 104 (2000) 9696–9703.
- [16] C. Bianchi, F. Porta, L. Prati, M. Rossi, *Top. Catal.* 13 (2000) 231–236.
- [17] L. Prati, M. Rossi, *Stud. Surf. Sci. Catal.* 110 (1997) 509–516.
- [18] S. Carrettin, P. McMorn, P. Johnston, K. Griffin, G.J. Hutchings, *Chem. Commun.* 7 (2002) 696–697.
- [19] K.M. Kosuda, A. Wittstock, C.M. Friend, M. Bäumer, *Angew. Chem. Int. Ed.* 51 (2012) 1698–1701.
- [20] V.V. Costa, M. Estrada, Y. Demidova, I. Prosvirin, V. Kriventsov, R.F. Cotta, S. Fuentes, A. Simakov, E.V. Gusevskaya, *J. Catal.* 292 (2012) 148–156.
- [21] A.V. Radha, P. Vishnu Kamath, G.N. Subbanna, *Mater. Res. Bull.* 38 (2003) 731–740.
- [22] M. Haruta, *J. New Mater. Electrochem. Syst.* 7 (2004) 163–172.
- [23] K. Itatani, K. Koizumi, S. Howell, A. Kishioka, M. Kinoshita, *J. Mater. Sci.* 23 (1988) 3405–3412.
- [24] V.V. Kriventsov, I.L. Simakova, A. Simakov, E. Smolentseva, F. Castillon, M. Estrada, E. Vargas, E.P. Yakimchuk, D.P. Ivanov, D.G. Aksenov, D.V. Andreev, B.N. Novgorodov, D.I. Kochubey, S. Fuentes, *Nucl. Instrum. Meth. Phys. Res. A* 603 (2009) 185–187.
- [25] S. Ivanova, V. Pitchon, Y. Zimmermann, C. Petit, *Appl. Catal. A* 298 (2006) 57–64.
- [26] K. Itatani, K. Koizumi, F.S. Howell, A. Kishioka, M. Kinoshita, *J. Mater. Sci.* 23 (1988) 3405–3412.
- [27] S. Ardzzone, C.L. Bianchi, M. Fadoni, B. Vercelli, *Appl. Surf. Sci.* 119 (1997) 253–259.
- [28] E. Longo, J.A. Varela, A.N. Senapeschi, J. Whittemore, *Langmuir* 1 (1985) 456–461.
- [29] A.A. Tsyganenko, V.N. Filimonov, *J. Struct. Chem.* 5 (1972) 477–487.
- [30] K. Nakamoto, *Infrared Spectra of Inorganic and Coordination Compounds* (Russian translation), Mir, Moscow, 1966.
- [31] P. Buftat, J.P. Borel, *Phys. Rev. A* 13 (1976) 2287–2298.
- [32] C.J. Jia, Y. Liu, H. Bongard, F. Schütt, *J. Am. Chem. Soc.* 132 (2010) 1520–1522.
- [33] J.F. Moulder, W.F. Stickle, P.E. Sobol, K.D. Bomben, *Handbook of X-ray Photoelectron Spectroscopy*, Perkin-Elmer Corporation, Physical Electronics Division, Eden Prairie, 1992, pp. 179.
- [34] [http://www.kcvps.ca/site/projects/chemistry\\_files/Spectroscopy%20Applets/benzyl%20alcohol/benzylAlcohol.html](http://www.kcvps.ca/site/projects/chemistry_files/Spectroscopy%20Applets/benzyl%20alcohol/benzylAlcohol.html)
- [35] [http://www.hanhonggroup.com/ir/ir\\_en/B33092.html](http://www.hanhonggroup.com/ir/ir_en/B33092.html)

- [36] [http://www.hanhonggroup.com/ir/ir\\_zh-cn/B34154.html](http://www.hanhonggroup.com/ir/ir_zh-cn/B34154.html)
- [37] V.R. Choudhary, D.K. Dumbre, *Top. Catal.* 52 (2009) 1677–1687.
- [38] I.S. Nielsen, E. Taarning, K. Egeblad, R. Madsen, C.H. Christensen, *Catal. Lett.* 116 (2007) 35–40.
- [39] F.Z. Su, J. Ni, H. Sun, Y. Cao, H.Y. He, K.N. Fan, *Chem. Eur. J.* 14 (2008) 7131–7135.
- [40] J.C.F. Rodríguez-Reyes, C.M. Friend, R.J. Madix, *Surf. Sci.* 606 (2012) 1129–1134.
- [41] M.A. Brown, Y. Fujimori, F. Ringleb, X. Shao, F. Stavale, N. Nilius, M. Sterrer, H.-J. Freund, *J. Am. Chem. Soc.* 133 (2011) 10668–10676.